G Model
CCLET 2989 1–5
ARTICLE IN PRESS

Chinese Chemical Letters xxx (2014) xxx–xxx

Contents lists available at ScienceDirect

Chinese Chemical Letters

journal homepage: www.elsevier.com/locate/cclet

Original article

High efficient probes with Schiff base functional receptors for hypochlorite sensing under physiological conditions

Q1 Yang-Yang Huang, Meng-Jia Wang, Zheng Yang, Meng-Yao She, Shu Wang, Ping Liu *, Jian-Li Li *, Zhen Shi

Ministry of Education Key Laboratory of Synthetic and Natural Functional Molecule Chemistry, College of Chemistry & Materials Science, Northwest University, Xi'an 710069, China

ARTICLE INFO

Article history:
Received 18 March 2014
Received in revised form 11 April 2014
Accepted 22 April 2014
Available online xxx

Keywords:
Fluorescent probe
Schiff base
Hypochlorite
Cinnamyl aldehyde
Cell imaging

ABSTRACT

A series of novel and convenient fluorescent probes with Schiff base functionality were presented for direct detection of OCl^- *via* the irreversible OCl^--promoted oxidation and hydrolyzation reaction in formation of the ring-opened product, fluorescein. Prominent high sensitivity, selectivity and anti-interference OCl^--induced fluorescence and color change over a wide range of tested metal ions performance were observed for each probe under physiological conditions, thus making the probes well suitable for sensing of OCl^- in living cells.

1. Introduction

Fluorescent probes have long been considered as ideal candidates for biological studies [1,2] because the detection process is non-sample-destructing and less cell-damaging, and the instrumentation required for fluorescent detection is relatively simple, the selectivity and sensitivity is high, and the dynamic range is broad. Fluorescent detection in combination with microscopy can provide results in real time with spatial resolution and is amenable to high throughput methodology [3]. Since Czarnik [4] firstly reported the spiro ring-opening reaction of xanthene derivatives, this pioneering work has stimulated the development of a wide range of probes utilized for metal ions [5], biological relevant ions and the recognition and detection of biomolecules [6]. Among the most attractive functional groups, the Schiff base moiety has demonstrated to be an ideal receptor with significantly improved sensitivity, and selectivity as well as fluorescent properties and has proven to be highly suitable for the detection of heavy and transition metal ions at physiological pH, as well as thiols and reactive oxygen species (ROS) [7].

Due to the crucial roles in a wide scope of biological processes, the ROS have gained significant scientific interest [8]. As playing critical roles in water treatment and in the immune system [9], hypochlorous acid (HOCl), usually existing as the hypochlorite ion (OCl^-) at physiological pH, have especially received a considerable amount of clinical, commercial, and academic attention. The importance of hypochlorite is reflected by the fact that abnormal levels of hypochlorite have been implicated in a series of human diseases, such as cardiovascular diseases, damage of human red blood cells, neuron degeneration, lung injury, kidney disease, and cancer [10]. Therefore, the design and synthesis of highly selective and sensitive functionalized fluorescent probes with Schiff base function based on xanthene derivatives that are capable of detecting hypochlorite in biological systems is of particular importance [11].

Herein we report the design and biological application of a series of efficient fluorescent probes **1**–**3** with fluorescein as the fluorophore and a Schiff base moiety as the receptor. The probes displayed remarkable selectivity and anti-interference performance to hypochlorite in $MeOH/H_2O$ (4:6, v/v) solution with an extremely low detection limit at physiological pH range, thus enabling facile imaging of hypochlorite in living cells.

2. Experimental

Absorbance spectra were performed on a Shimadzu UV-1700 spectrophotometer. Fluorescent spectra measurements were performed on a Hitachi F-4500 fluorescent spectrophotometer.

* Corresponding authors.
E-mail address: lijianli@nwu.edu.cn (J.-L. Li).

http://dx.doi.org/10.1016/j.cclet.2014.05.011
1001-8417/

Please cite this article in press as: Y.-Y. Huang, et al., High efficient probes with Schiff base functional receptors for hypochlorite sensing under physiological conditions, Chin. Chem. Lett. (2014), http://dx.doi.org/10.1016/j.cclet.2014.05.011

X-ray crystal data were collected on the Bruker Smart APEX II CCD diffractometer. Elemental analyses were measured on a Vario EL III analyzer. IR spectra were acquired on the Bruker Tensor 27 spectrometer in KBr disks. Mass spectra were performed on the Bruker micrOTOF-Q II ESI-Q-TOF LC/MS/MS Spectrometer. NMR spectra were recorded on the Varian Inova-400 MHz spectrometer (at 400 MHz for ^{1}H and 100 MHz for ^{13}C). The chemicals and reagents were obtained from Sigma-Aldrich Co., LLC. Analytical thin layer chromatography was performed using Merck 60 GF254 silica gel coated glass plates. Silica gel (0.200–0.500 mm, 60A, J&K Scientific Ltd.) was used for column chromatography.

Synthesis of the probes: Fluorescein hydrazide was synthesized according to Ref. [12]. Fluorescein hydrazine (3.46 g, 0.01 mol) was then dissolved in 50 mL ethanol. The cinnamyl aldehydes (0.01 mol) were added in 30 min. The reaction mixture was refluxed for 12 h. After cooling to the room temperature, the solvent was evaporated and then washed with anhydrous ether to obtain a white or light yellow powder.

Probe **1**: White powder. mp: 289–290 °C. Anal. Calcd. for $C_{29}H_{20}N_2O_4$: H: 4.38, C: 75.64, N: 6.08. Found: H: 4.36, C: 75.69, N: 6.09. ^{1}H NMR (400 MHz, DMSO-d_6, TMS): δ 9.92 (s, 2H), 8.93 (d, 1H, J = 9.1 Hz), 7.88 (d, 1H, J = 7.2 Hz), 7.58 (dd, 4H, J = 14.4, 7.3 Hz), 7.31 (dd, 3H, J = 15.0, 7.5 Hz), 7.04 (d, 1H, J = 7.0 Hz), 6.95 (d, 1H, J = 16.0 Hz), 6.76 (dd, 1H, J = 15.9, 9.2 Hz), 6.64 (s, 2H), 6.49 (dd, 4H, J = 21.3, 8.6 Hz). ^{13}C NMR (100 MHz, DMSO-d_6, TMS): δ 163.9, 158.5, 153.0, 151.9, 151.2, 140.4, 135.6, 133.9, 129.0, 128.7, 128.4, 128.0, 127.3, 126.2, 123.6, 123.2, 112.4, 110.0, 102.6, 65.2. MS (ESI) m/z 461.1489 $[M+H]^+$, Calcd. for $C_{29}H_{20}N_2O_4$ 460.1423.

Probe **2**: White powder. mp: 277–278 °C. Anal. Calcd. for $C_{30}H_{22}N_2O_4$: H: 4.67, C: 75.94, N: 5.90. Found: H: 4.66, C: 75.99, N: 5.89. ^{1}H NMR (400 MHz, DMSO-d_6, TMS): δ 9.90 (s, 2H), 8.85 (s, 1H), 7.90 (d, 1H, J = 7.3 Hz), 7.69–7.55 (m, 2H), 7.37 (d, 4H, J = 6.5 Hz), 7.28 (s, 1H), 7.13 (d, 1H, J = 7.3 Hz), 6.67 (d, 3H, J = 18.6 Hz), 6.46 (s, 4H), 1.80 (s, 3H). ^{13}C NMR (100 MHz, DMSO-d_6, TMS): δ 163.3, 158.6, 154.5, 152.4, 150.2, 137.8, 136.1, 134.8, 133.8, 129.4, 129.1, 128.4, 128.1, 127.8, 123.9, 123.2, 112.3, 110.4, 102.5, 65.4, 11.9. MS (ESI) m/z 475.1652 $[M+H]^+$, Calcd. for $C_{30}H_{22}N_2O_4$ 474.1582.

Probe **3**: Yellow powder. mp: 284–285 °C. Anal. Calcd. for $C_{29}H_{19}BrN_2O_4$: H: 3.55, C: 64.58, N: 5.19. Found: H: 3.54, C: 64.59, N: 5.21. ^{1}H NMR (400 MHz, DMSO-d_6, TMS): δ 9.91 (s, 2H), 9.08 (s, 1H), 7.92 (d, 1H, J = 7.2 Hz), 7.77 (d, 2H, J = 7.1 Hz), 7.67–7.56 (m, 3H), 7.40 (d, 3H, J = 7.6 Hz), 7.15 (d, 1H, J = 7.3 Hz), 6.64 (s, 2H), 6.47 (s, 4H). ^{13}C NMR (100 MHz, DMSO-d_6, TMS): δ 163.6, 158.6, 152.4, 150.3, 148.9, 139.0, 134.5, 134.2, 129.8, 129.3, 129.0, 128.4, 128.0, 124.0, 123.4, 120.6, 112.3, 110.1, 102.5, 65.8. MS (ESI) m/z 537.0463 $[M-H]^-$, Calcd. $C_{29}H_{19}BrN_2O_4$ 538.0528.

Synthesis of the product of probe **1** upon addition of OCl^-: Probe **1** (0.46 g, 1 mmol) was dissolved in 20 mL ethanol. The 1.0 mL of 30% NaOCl solution was then added. The reaction mixture was refluxed for 1 h. After cooling to the room temperature, the mixture was filtrated and solvent evaporated under reduced pressure and the resulting powder was purified by column chromatography on silica gel (eluent: ethyl acetate only) yielding an orange powder. ^{1}H NMR (400 MHz, DMSO-d_6, TMS): δ 7.80 (d, 1H, J = 8.2 Hz), 7.54 (s, 3H), 7.30 (d, 4H, J = 7.4 Hz), 6.81 (d, 2H, J = 7.9 Hz), 6.10 (s, 1H), 6.01 (s, 1H). MS (ESI) m/z 333.0757 $[M+H]^+$, Calcd. for $C_{20}H_{12}O_5$ 332.0685.

General procedure: The stock solutions of probes were prepared at 500 μmol/L concentration. The solutions of ions, including LiCl, NaCl, KCl, $BaCl_2$, $MgCl_2$, $CaCl_2$, $CdCl_2$, $MnCl_2$, $CoCl_2$, $ZnCl_2$, $NiCl_2$, $CuCl_2$, $HgCl_2$, $PbCl_2$, $CrCl_3$, $FeCl_3$, $AlCl_3$, $SnCl_4$, $NaNO_3$, Na_2CO_3, $NaHCO_3$, Na_2SO_4, Na_3PO_4, Na_2HPO_4, NaH_2PO_4, NaOAc, H_2O_2, and NaOCl, were also prepared at 500 μmol/L in $MeOH/H_2O$ (4:6, v/v). The fluorescence intensity was recorded at 533 nm with an excitation wavelength at 490 nm. The absorption data were recorded at 517 nm.

Crystal growth and conditions: White single crystals of the probes were obtained at room temperature from a mixed solution of CH_2Cl_2–CH_3CN by slow evaporation and then mounted on the goniometer of a single crystal diffractometer. The crystal data have been collected at 296 K by using Mo $K\alpha$ radiation (λ = 0.710713 Å) and the φ/ω scan mode and Analyzed for Lorentz and polarization effect (SADABS). The structure was solved using the direct method and refined by full-matrix least-squares fitting on F^2 by SHELX-97.

Fluorescent imaging: Human Osteosarcoma MG-63 cells were cultured in Dulbecco's Modified Eagle Medium (DMEM) supplemented with 10% FBS, at 37 °C in a humidified atmosphere of 5% CO_2 and 95% air. The cells were then cultured for 2 h until they plated on glass-bottomed dishes. The growth medium was then removed and the cells were washed with DMEM without FBS and incubated with 20 μmol/L of the probes for 4 h at 37 °C, washed three times with PBS and imaged. Then the cells were supplemented with 200 μmol/L NaOCl in the growth medium for 4 h at 37 °C and imaged [13].

3. Results and discussion

The probes were prepared by the synthetic route outlined in Scheme 1. The facile formylation reaction of fluorescein and hydrazine hydrate gave fluorescein hydrazide, which was further treated with cinnamyl aldehydes in EtOH solution at reflux temperature to yield the target probes. The probes were characterized by X-ray single crystal analysis in combination with elemental analysis, IR, NMR, and MS spectra. The X-ray crystal structural investigation clearly showed the special Schiff base functional group (Fig. 1). The structural differences between the probes are a result of the different substitution groups, which were further investigated to have obvious effects on the fluorescent properties.

We commenced our investigation by first verification of the sensing media. The combination of $MeOH/H_2O$ (4:6, v/v) was proved to be highly efficient (Figs. S1–S3 in Supporting information). The selective properties of the probes were then examined under simulated physiological conditions (PBS buffer, pH 7.4) based on the investigation of pH responses using the solutions with pH values from 1.7 to 13.0 (Figs. S4–S6 in Supporting information). The probes exhibited similar high selectivity toward OCl^- (Fig. 2, Red bars, Fig.S7–S9 in Supporting information) among the various testing ions including Li^+, Na^+, K^+, Mg^{2+}, Ba^{2+}, Ca^{2+}, Mn^{2+}, Ni^{2+}, Hg^{2+}, Co^{2+}, Zn^{2+}, Pb^{2+}, Cu^{2+}, Cd^{2+}, Fe^{3+}, Al^{3+}, Cr^{3+}, Sn^{4+}, SO_4^{2-}, Cl^-, CO_3^{2-},

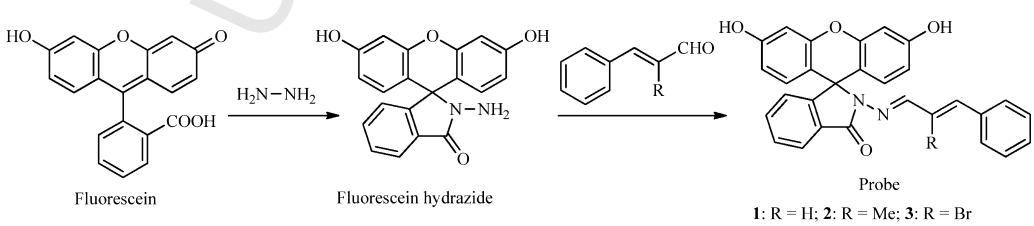

Scheme 1. Synthesis of the probes.

Please cite this article in press as: Y.-Y. Huang, et al., High efficient probes with Schiff base functional receptors for hypochlorite sensing under physiological conditions, Chin. Chem. Lett. (2014), http://dx.doi.org/10.1016/j.cclet.2014.05.011

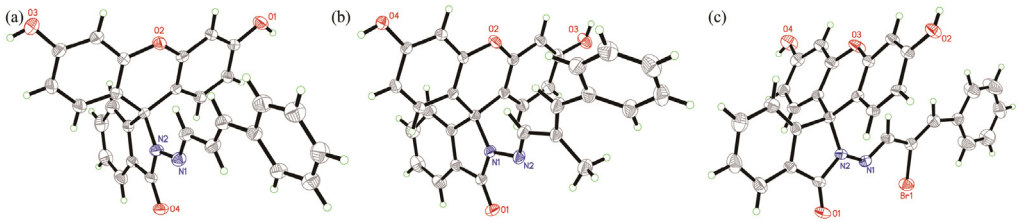

Fig. 1. Molecular structures of probes.

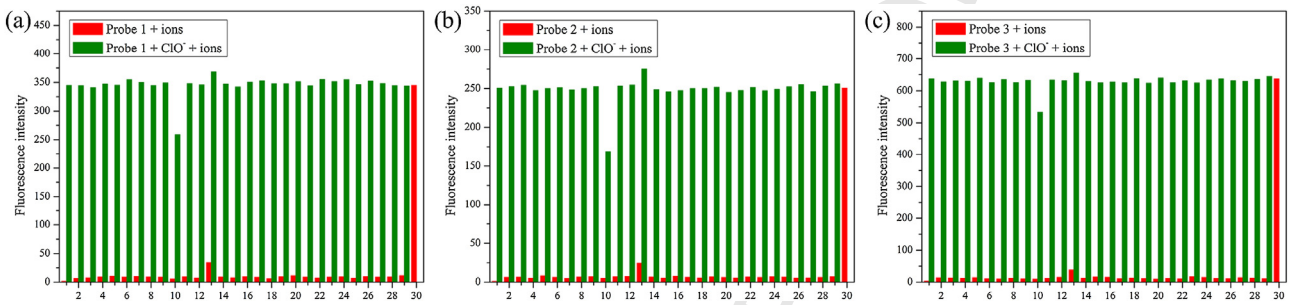

Fig. 2. Fluorescence intensity changes of the probes (20 μmol/L) upon addition of various ions (10 equiv.) in MeOH/H_2O (4:6, v/v) solution. Red bars represent the fluorescence responses of the probes to the ions of interest: 1. blank, 2. Li^+, 3. Na^+, 4. K^+, 5. Mg^{2+}, 6. Ca^{2+}, 7. Al^{3+}, 8. Cr^{3+}, 9. Mn^{2+}, 10. Fe^{3+}, 11. Co^{2+}, 12. Ni^{2+}, 13. Cu^{2+}, 14. Zn^{2+}, 15. Cd^{2+}, 16. Sn^{4+}, 17. Ba^{2+}, 18. Hg^{2+}, 19. Pb^{2+}, 20. Cl^-, 21. SO_4^{2-}, 22. NO_3^-, 23. PO_4^{3-}, 24. HPO_4^{2-}, 25. $H_2PO_4^-$, 26. CO_3^{2-}, 27. HCO_3^-, 28. OAc^-, 29. H_2O_2, 30. OCl^-. The green bars represent the subsequent addition of 200 μmol/L OCl^- to the above solutions.(For interpretation of the references to color in this text, the reader is referred to the web version of the article.)

Q3

HCO_3^-, NO_3^-, OAc^-, PO_4^{3-}, HPO_4^{2-}, $H_2PO_4^-$, H_2O_2, and OCl^-. By successively adding OCl^- to the solutions of each probes in the presence of other ions, a series of competition experiments were investigated. The results revealed that the addition of the commonly co-existent ions did not significantly result in interference, although Fe^{3+} induced a slight fluorescent quenching (Fig. 2, cation 10, Green bars).

Absorption and fluorescent titrations were then conducted in MeOH/H_2O solution (4:6, v/v, PBS buffer). As expected, the probe solution was colorless without OCl^-, while the obvious color changed from colorless to yellow occurred upon addition of OCl^- with the absorbance at 517 nm for all probes (Figs. S13–S18 in Supporting information). On the other hand, the fluorescent emission wavelength of the probes all appeared at 533 nm upon addition of OCl^-, indicating the occurrence of the ring-opening process which was supposed to be induced by the irreversible OCl^- promoted oxidation and hydrolyzation reaction in formation of the ring-opened product of fluorescein according to Ref. [14]. The mechanism was also supported by the ^1H NMR spectra in which the product displayed significant differences from probe **1**, but quite close similarity to fluorescein (Fig. S31 in Supporting information). In addition, the mass spectral data, upon addition of OCl^- manifested the peaks at 330.0757 ($[M+H]^+$, probe **1** upon addition of OCl^-, Fig. S32 in Supporting information), 330.0744 ($[M+H]^+$, probe **2** upon addition of OCl^-, Fig. S33 in Supporting information), and 330.0753 ($[M+H]^+$, probe **3** upon addition of OCl^-, Fig. S34 in Supporting information) which also produced powerful proofs for the predicted product of fluorescein ($C_{20}H_{12}O_5$, Calcd. 332.0685).

The emission intensity reached its maximum when 10 equiv. of OCl^- was added. The fluorescent quantum efficiency were calculated to be 0.22 (probe **1**), 0.15 (probe **2**) and 0.31 (probe **3**), respectively, by using fluorescein as the standard. Furthermore, the linear dependence of the fluorescence intensity on the concentration of OCl^- in the range of 0–200 μmol/L (Figs. S10–S12), and the lower detection limit of 2 μmol/L also provided powerful evidence for the possibility of the use of the probes in quantitative detection of OCl^- (Fig. 3). Although the R groups caused no changes in absorption and emission wavelengths, the fluorescence intensity and absorbance were greatly affected by

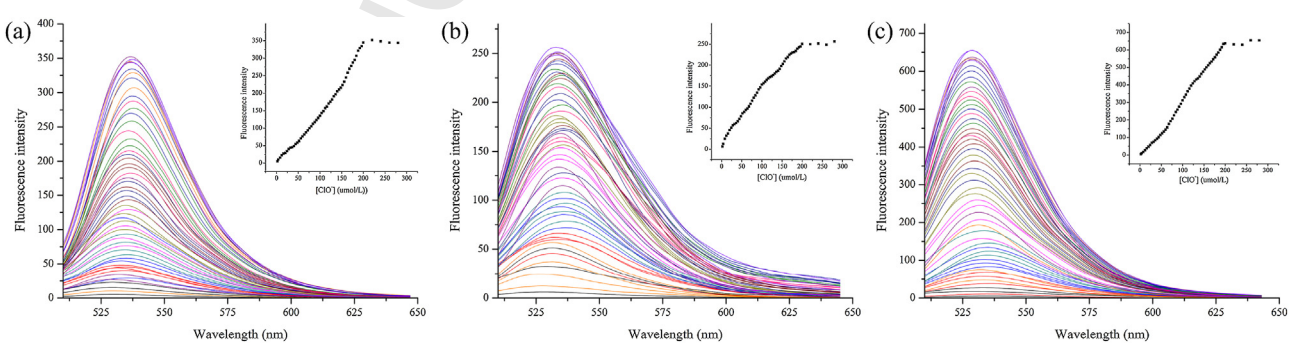

Fig. 3. Fluorescent titration of probe **1** (a), probe **2** (b) and probe **3** (c) in MeOH/H_2O (4:6, v/v) solution (20 μmol/L) in the presence of OCl^- ions of different concentrations (0–10 equiv.). Inset: changes of the fluorescence intensities at 533 nm as the function of OCl^- concentration.

Please cite this article in press as: Y.-Y. Huang, et al., High efficient probes with Schiff base functional receptors for hypochlorite sensing under physiological conditions, Chin. Chem. Lett. (2014), http://dx.doi.org/10.1016/j.cclet.2014.05.011

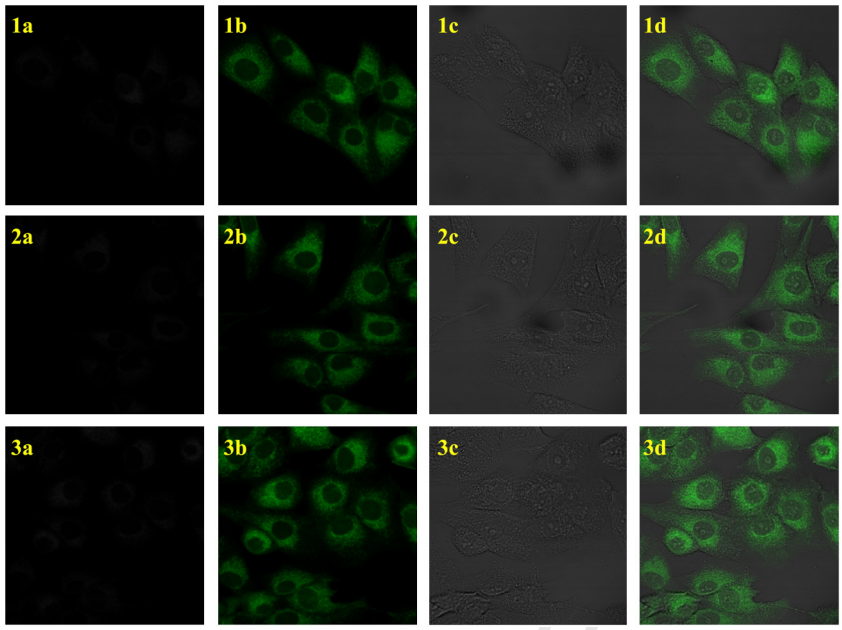

Fig. 4. (1–3a) Fluorescent images of Human Osteosarcoma MG-63 cells incubated with 20 μmol/L probes for 4 h at 37 °C. (1–3b) Cells supplemented with 10 equiv. of OCl^- at 37 °C and then loaded with the probes for 4 h in the same growth media. (1–3c) Bright field images of the cells incubated with OCl^- and the probes. The overlay image of (b) and (c) is shown in (d).

different substituent groups. It is clear that the effect of a heavy atom induced a significant enhancement in the fluorescent intensity and absorbance, while the alkyl groups weakened both the intensity and the absorbance, thus making probe **3** superior to the other ones. The investigation of the effect of the R group provides significant contributions in understanding the function of the substituent group in the receptor moiety, thus contributing to the utilization in the screening of effective recognition moieties in the design and application of probes.

To further evaluate the potential application of the probes for tracking of OCl^- in living cells, fluorescent imaging for OCl^- was carried out in combination with confocal laser scanning microscopy. No intracellular fluorescence was observed (Fig. 4a) when cultured Human Osteosarcoma MG-63 cells were incubated with the probes in the medium for 4 h at 37 °C. In contrast, significant fluorescence increases were monitored when the cells were supplemented with 10 equiv. of OCl^- at 37 °C and then loaded with the probes for 4 h in the same growth media (Fig. 4b). Moreover, the cells were proved to be viable throughout the imaging experiments (Fig. 4c) and the fluorescence signals were observed to be localized in the cytosol (Fig. 4d). This preliminary investigation suggested that the probes are cell membrane permeable and can be efficiently used for sensing of OCl^- in living cells.

4. Conclusion

In summary, we have demonstrated a series of novel probes with special Schiff base functional group for direct detection of OCl^- in which switchable fluorescence was achieved from the irreversible OCl^--promoted oxidation and hydrolyzation reaction in the formation of the ring-opened product, fluorescein. The probes showed remarkable fluorescence enhancement in response to OCl^- with significantly high sensitivity and selectivity. The probes have been proven to be well suitable for tracking of OCl^- in living cells, thus providing ideal candidates in understanding the basis of the biological importance of OCl^- in physiological progresses.

Acknowledgments

The work was supported by National Natural Science Foundation of China (Nos. 21272184, 20972124, 21143010 and J1210057), the Shaanxi Provincial Natural Science Fund Project (No. 2012JQ2007), the Northwest University Science Foundation for Postgraduate Students (Nos. YZZ12030, YZZ13042), and the Chinese National Innovation Experiment Program for University Students (No. 201210697011).

Appendix A. Supplementary data

Supplementary data associated with this article can be found, in the online version, at http://dx.doi.org/10.1016/j.cclet.2014.05.011.

References

[1] (a) M. Vendrell, D.T. Zhai, J.C. Er, Y. Chang, Combinatorial strategies in fluorescent probe development, Chem. Rev. 112 (2012) 4391–4420;
(b) Y.Y. Huang, M.J. Wang, M.Y. She, et al., Recent progress in the fluorescent probe based on spiro ring opening of xanthenes and related derivatives, Chin. J. Org. Chem. 34 (2014) 1–25;
(c) L. Chen, Q. Zhao, X.Y. Zhang, G.H. Tao, Determination of silver ion based on the redshift of emission wavelength of quantum dots functionalized with rhodanine, Chin. Chem. Lett. 25 (2014) 261–264;
(d) Q. Liu, L. Xue, D.J. Zhu, et al., Highly selective two-photon fluorescent probe for imaging of nitric oxide in living cells, Chin. Chem. Lett. 25 (2014) 19–23.
[2] (a) H. Woo, S. Cho, Y. Han, et al., Synthetic control over photoinduced electron transfer in phosphorescence zinc sensors, J. Am. Chem. Soc. 135 (2013) 4771–4787;
(b) X.Y. Qu, C.J. Li, H.C. Chen, A red fluorescent turn-on probe for hydrogen sulfide and its application in living cells, Chem. Commun. 49 (2013) 7510–7512;
(c) M.Z. Tian, L.B. Liu, Y.J. Li, et al., An unusual OFF–ON fluorescence sensor for detecting mercury ions in aqueous media and living cells, Chem. Commun. 50 (2014) 2055–2057;
(d) W.T. Yin, H. Cui, Z. Yang, et al., Facile synthesis and characterization of rhodamine-based colorimetric and off–on fluorescent chemosensor for Fe^{3+}, Sens. Actuators B: Chem. 157 (2011) 675–680;
(e) M.Y. She, Z. Yang, B. Yin, et al., A novel rhodamine-based fluorescent and colorimetric "off–on" chemosensor and investigation of the recognizing behavior

towards Fe^{3+}, Dyes Pigments 92 (2012) 1337–1343;
(f) Q. Liu, G.P. Li, D.J. Zhu, et al., Design of quinolone-based fluorescent probe for the ratiometric detection of cadmium in aqueous media, Chin. Chem. Lett. 24 (2013) 479–482.

[3] (a) Z.Q. Guo, S. Park, J. Yoon, I. Shin, Recent progress in the development of near-infrared fluorescent probes for bioimaging applications, Chem. Soc. Rev. 43 (2014) 16–29;
(b) Z. Yang, L.K. Hao, B. Yin, et al., Six-membered spirocycle triggered probe for visualizing Hg^{2+} in living cells and bacteria-EPS-mineral aggregates, Org. Lett. 15 (2013) 4334–4337;
(b) Z. Yang, L.K. Hao, B. Yin, et al., Six-membered spirocycle triggered probe for visualizing Hg^{2+} in living cells and bacteria-EPS-mineral aggregates, Org. Lett. 15 (2013) 4334–4337.

[4] V. Dujols, F. Ford, A.W. Czarnik, A long-wavelength fluorescent chemodosimeter selective for Cu(II) ion in water, J. Am. Chem. Soc. 119 (1997) 7386–7387.

[5] H.N. Kim, M.H. Lee, H.J. Kim, et al., A new trend in rhodamine based chemosensors: application of spirolactam ring-opening to sensing ions, Chem. Soc. Rev. 37 (2008) 1465–1472.

[6] X.Q. Chen, T. Pradhan, F. Wang, et al., Fluorescent chemosensors based on spiroring-opening of xanthenes and related derivatives, Chem. Rev. 112 (2012) 1910–1956.

[7] X.H. Li, X.H. Gao, W. Shi, H.M. Ma, Design strategies for water-soluble small molecular chromogenic and fluorogenic probes, Chem. Rev. 114 (2014) 590–659.

[8] (a) S. Kundu, P. Ghosh, S. Datta, et al., Oxidative stress as a potential biomarker for determining disease activity in patients with rheumatoid arthritis, Free Radical Res. 46 (2012) 1482–1489;
(b) D.M. Tabima, S. Frizzell, M.T. Gladwin, Reactive oxygen and nitrogen species in pulmonary hypertension, Free Radical Biol. Med. 2 (2012) 51970–51986.

[9] M.J. Gray, W.Y. Wholey, U. Jakob, Bacterial responses to reactive chlorine species, Annu. Rev. Microbiol. 67 (2013) 141–160.

[10] (a) M.R. Ramsey, N.E. Sharpless, ROS as a tumor suppressor? Nat. Cell Biol. 8 (2006) 1213–1215;
(b) C. Nussbaum, A. Klinke, M. Adam, et al., Myeloperoxidase: a leukocyte-derived protagonist of inflammation and cardiovascular disease, Antioxid. Redox Sign. 18 (2013) 692–713.

[11] (a) Q.L. Xu, K. Lee, S. Lee, et al., A highly specific fluorescent probe for hypochlorous acid and its application in imaging microbe-induced HOCl production, J. Am. Chem. Soc. 135 (2013) 9944–9949;
(b) X.J. Wu, Z. Li, L. Yang, et al., A self-referenced nanodosimeter for reaction based ratiometric imaging of hypochlorous acid in living cells, Chem. Sci. 4 (2013) 460–467;
(c) M. Emrullahoğlu, M. Üçüncü, E. Karakus, A BODIPY aldoxime-based chemodosimeter for highly selective and rapid detection of hypochlorous acid, Chem. Commun. 49 (2013) 7836–7838;
(c) M. Emrullahoğlu, M. Üçüncü, E. Karakus, A BODIPY aldoxime-based chemodosimeter for highly selective and rapid detection of hypochlorous acid, Chem. Commun. 49 (2013) 7836–7838.

[12] L. Yuan, W.Y. Lin, Z.M. Cao, L.L. Long, J.Z. Song, Photocontrollable analyte-responsive fluorescent probes: a photocaged copper-responsive fluorescence turn-on probe, Chem. Eur. J. 17 (2011) 689–696.

[13] (a) Z. Yang, M.Y. She, J. Zhang, et al., Highly sensitive and selective rhodamine Schiff base "off–on" chemosensors for Cu^{2+} imaging in living cells, Sens. Actuators B: Chem. 176 (2013) 482–487;
(b) Z. Yang, M.Y. She, B. Yin, et al., Three rhodamine-based "off–on" chemosensors with high selectivity and sensitivity for Fe^{3+} imaging in living cells, J. Org. Chem. 77 (2012) 1143–1147.

[14] (a) X.Q. Chen, X.C. Wang, S.J. Wang, et al., A highly selective and sensitive fluorescence probe for the hypochlorite anion, Chem. Eur. J. 14 (2008) 4719–4724;
(b) G.W. Chen, F.L. Song, J.Y. Wang, et al., FRET spectral unmixing: a ratiometric fluorescent nanoprobe for hypochlorite, Chem. Commun. 48 (2012) 2949–2951.

Please cite this article in press as: Y.-Y. Huang, et al., High efficient probes with Schiff base functional receptors for hypochlorite sensing under physiological conditions, Chin. Chem. Lett. (2014), http://dx.doi.org/10.1016/j.cclet.2014.05.011